

Development of a high-efficiency DF-STEM detector

T. Kaneko¹, A. Saitow¹, T. Fujino¹, E. Okunishi¹ and H. Sawada¹

¹ JEOL Ltd. 1-2 Musashino 3-Chome, Akishima, Tokyo 196-8558, Japan

E-mail: takekane@jeol.co.jp

Abstract. We experimentally evaluated the signal intensity produced by an electron on three types of scintillators. A powder scintillator showed high efficiency at a low accelerating voltage, whereas a single crystal scintillator showed high efficiency at higher accelerating voltages. On the basis of these characteristics, for a dark-field (DF) scanning transmission electron microscope (STEM), we have developed a new hybrid type scintillator, which consisted of a powder deposited on a single crystal substrate. The luminescent quantum efficiency of the hybrid scintillator was measured to be twice as large as that of the single crystal type detector at 60 kV and was about 8 times higher than that of the powder type detector at 300 kV. The developed detector has advantages of powder and single crystal type detectors, and covers the observation at the accelerating voltages from low to high voltages. Especially, it is useful for low voltage observations of carbon-based materials consisted of few atomic layers that produces weak scattering of electron.

1. Introduction

High-resolution dark-field (DF) imaging with an aberration corrected scanning transmission electron microscope (STEM) has been widely used for structural analysis in materials science. A conventional DF-STEM detector consists of a scintillator, a glass light pipe, and a photomultiplier tube (PMT). The scintillator of the DF-STEM detector is selectable either a powder scintillator or a single crystal scintillator. Y_2SiO_5 doped with Ce (P47) is used for the powder scintillator. And, the single crystal scintillator is made of yttrium aluminum garnet (YAG) or yttrium aluminum perovskite (YAP). Faruqi and Tyrell investigated the relationship between the thickness of the powder scintillator and the accelerating voltage [1]. In their study, a powder scintillator was reported to show a maximum of efficiency at a particular accelerating voltage. The accelerating voltage showing the maximum efficiency depends on the thickness of the powder scintillator. A YAG single crystal scintillator has been used for the charge-coupled device camera of transmission electron microscopy [2-4]. The YAP scintillator is mostly used for the DF-STEM detector, because its wavelength of the luminescence is sensitive for a conventionally commercialized PMT [5, 6].

Most recently, observations at low accelerating voltages have been widely popular for carbon-based materials such as carbon nanotubes or graphenes [7-9], to reduce knock-on damage due to irradiation of an electron beam. These materials generally produce a small amount of scattered

¹ To whom any correspondence should be addressed.



electrons for the DF-STEM detector because they are composed of a few atomic layers. A DF-STEM detector of high-efficiency is longed to obtain an STEM image with a better signal-to-noise ratio. In this study, we explain the characters of a new highly-efficient DF-STEM detector. And we show the DF-STEM image taken at a lower accelerating voltage using the detector.

2. Experimental and methods

Three scintillators (P47 powder, YAP single crystal, and hybrid scintillators) were tested, as described below. The intensity of the signal per electron was measured, on each scintillator at accelerating voltages ranging from 30 kV to 300 kV. An electron beam was focused and scanned on the scintillator screen by adjusting the excitations of several lenses to see the map of the signal intensity. The probe current was measured using a Faraday cage, and the number of electrons per a unit time was calculated using the elementary charge of an electron. The Gatan DigiScanTM system was employed to obtain an average of the digitally counted intensity on each scintillator. The intensity per electron on each scintillator was calculated as a quotient of averaged the digital counts on the image of the scintillator divided by the number of electrons.

Figure 1(a) shows the schematic of the detector, and an intensity map of the scintillator, which shows a flatness of detection, is displayed in Fig. 1(b). In the conventionally in-use DF-STEM detectors, the image of the scintillator lacked uniformity around the center hole of the detector [10-16]. Whereas, for the developed DF-STEM detector, we reduced this non-uniformity by redesigning the structure of the DF-STEM detector, thereby achieving a relatively uniform signal intensity over the scintillator, as shown in Fig. 1(b).

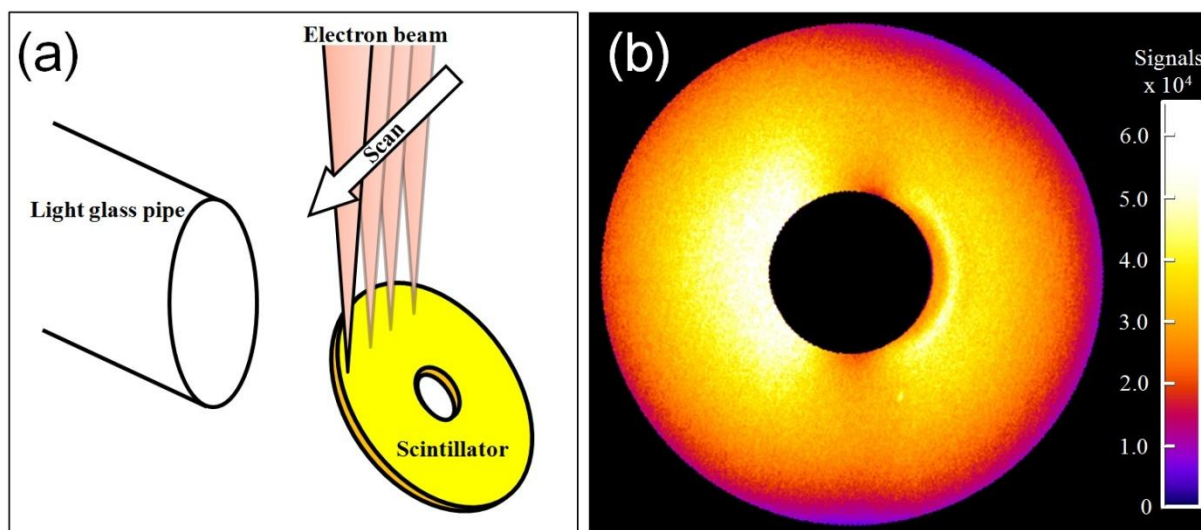


Figure 1. (a) Schematic of the DF-STEM detector and scanning method of the scintillator. (b) Scanning image of the scintillator.

3. Results and discussion

3.1. Development of the hybrid detector

Scanning images of the scintillators were obtained at several accelerating voltages, and their efficiencies were measured. Figure 2 shows the plotted signal intensity per electron as a function of the accelerating voltage for the three scintillators. The YAP single crystal and the P47 powder scintillators are used in the conventional detectors. The thicknesses of scintillators for the YAP single crystal and the P47 powder were 0.5 mm and 30 μm , respectively. The efficiency (signal intensity per electron) of the YAP single crystal scintillator increases as the accelerating voltage increases. The efficiency of the YAP single crystal scintillator is higher than that of P47 powder scintillator at

accelerating voltages greater than 100 kV. On the other hand, the efficiency of the P47 powder scintillator is relatively uniform with respect to that of the YAP single crystal scintillator. P47 shows a maximum efficiency at 60 kV. For accelerating voltages less than 60 kV, the signal intensity of the P47 powder scintillator is higher than that of the YAP single crystal scintillator.

These characteristics are attributed to the forms and thicknesses of the materials of scintillators. In the YAP single crystal scintillator, the electron produces photons until the electron energy becomes lower than the threshold energy to produce a photon. We can say that the number of photons produced by electron is roughly proportional to the accelerating voltage. The thickness of YAP single crystal scintillator is sufficiently thick for electrons of high energy, resulting in more photons produced in a thick YAP single crystal scintillator than thin P47 powder scintillator at accelerating voltages higher than 60 kV. On the other hand, in scintillator made of a thin layer of P47 powder, emitted photon tends to encounter to the surface of the powder particle with high incident angle, because of small curvature of powder particles. The high incident angle leads, the higher escape probability of photons than thick and scintillation crystal that has wide and flat surfaces, resulting in higher emission of photons for powder scintillator. And most of energy of incident electrons less than 60 kV is consumed in the layer. Thus, the scintillator of powder is superior than that made of single crystal scintillator at accelerating voltage below 60 kV.

By combining the advantage of these scintillators, we built a hybrid scintillator, which is made of deposited a 30- μm -thick P47 powder layer on a 0.5-mm-thick YAP single crystal substrate. The efficiency of the developed hybrid scintillator is also plotted in Fig. 2, as a function of the accelerating voltage. When an electron hits the P47 powder scintillator at the surface, the hybrid scintillator produces luminescence, and the emitted photons are transmitted through the transparent YAP single crystal scintillator. Moreover, the transmitted electrons or X-rays passing through P47 produce another luminescence in the YAP single crystal. Thus, the total efficiency is the sum of these two scintillators, resulting in the higher efficiency of the developed detector with respect to the two conventional scintillators at each accelerating voltage. The signal intensity of the hybrid scintillator was about 8 times as large as the intensity of the P47 powder scintillator at 300 kV. Furthermore, the luminescent quantum efficiency of the hybrid scintillator was twice as large as that of the YAP single crystal scintillator at 60 kV.

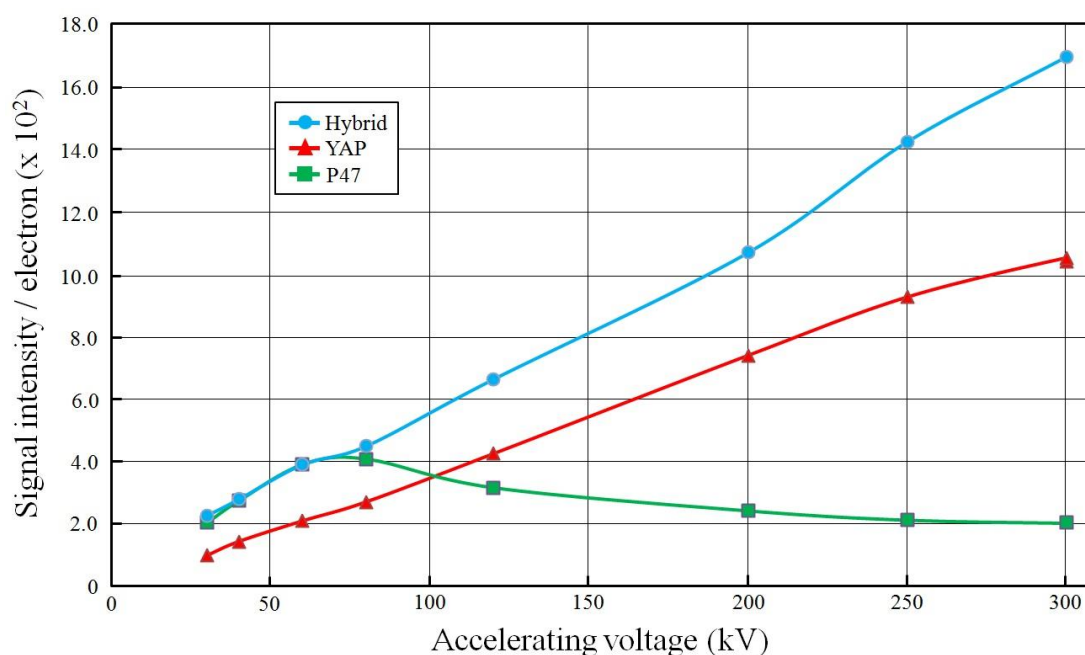


Figure 2. Signal intensity per electron of three scintillators plotted as a function of the accelerating voltage.

3.2. Observation of the STEM image of graphene

Using the developed hybrid detector, we performed STEM observation of graphene at 80 kV, using an aberration-corrected microscope (JEM-ARM200F) equipped with a cold field emission gun. Figure 3 shows the DF-STEM images with a probe current of 22 pA and a convergence semi-angle of 33 mrad. The detecting angle for the DF-STEM detector was set to range from 54 mrad to 216 mrad in this observation. The dwell time for a pixel and the number of pixels for the STEM image were 19.3 μ s and 512 \times 512 pixels, respectively. Single carbon atoms in mono atomic sheet were clearly observed as a bright dot. The intensity profile taken from the area indicated by a dotted rectangle is shown in Fig. 3(b). C-C atoms separated by 0.14 nm were imaged with sufficient dips between them.

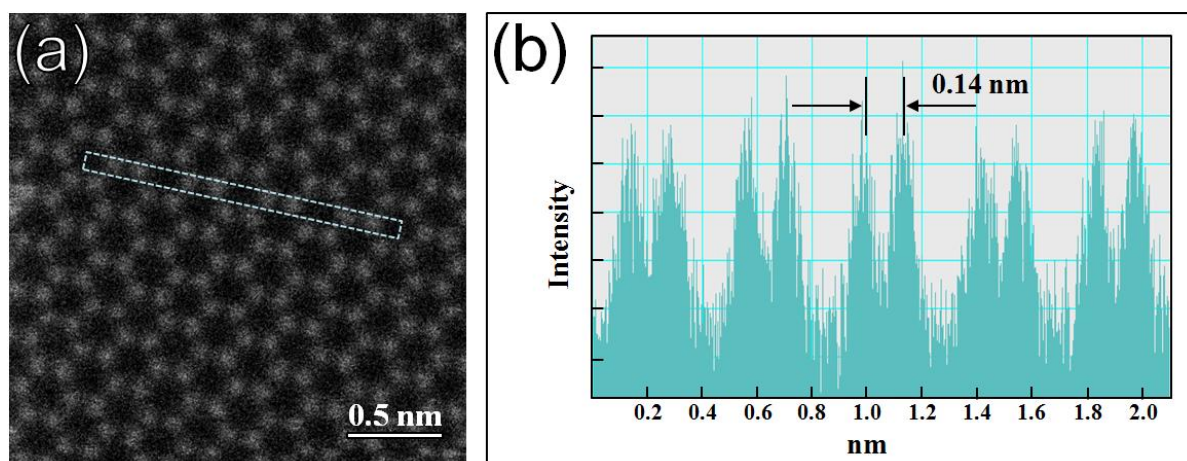


Figure 3. (a) DF-STEM image of graphene. (Raw data) (b) Intensity profile of dotted rectangular area.

4. Summary

A DF-STEM detector was developed by combining the powder and transparent crystalline scintillators. Experimental measurements showed that the developed hybrid detector had higher efficiency than the conventional detectors at accelerating voltages ranging from 30 kV to 300 kV. A single carbon atom in a mono atomic sheet of graphene was successfully imaged with new hybrid detector at 80 kV, using an atomic resolution electron microscope (JEM-ARM200F).

Acknowledgements

This work was supported by JST under the Research Accelerating Program (2012–2016).

The authors thank Dr. U. Mirsaidov of National University of Singapore for providing us the graphene sample.

References

- [1] Faruqi A R and Tyrell G C 1999 *Ultramicroscopy* **76** 69
- [2] Daberkow I, Herrmann K H, Liu L and Rau W D 1991 *Ultramicroscopy* **38** 215
- [3] Nishi R, Yoshida K, Takaoka A and Katsuta T 1996 *Ultramicroscopy* **62** 271
- [4] Zuo J M 2000 *Microscopy Research and Technique* **49** 245
- [5] Haider M 1989 *Ultramicroscopy* **28** 240
- [6] Kirkland E J and Thomas M G 1996 *Ultramicroscopy* **62** 79
- [7] Suenaga K and Koshino M 2010 *Nature* **468** 1088
- [8] Krivanek O L, Dellby N, Murfitt M F, Chisholm M F, Pennycook T J, Suenaga K and Nicolosi V 2010 *Ultramicroscopy* **110** 935
- [9] Zan R, Ramasse Q M, Bangert U and Novoselov K S 2012 *Nano Lett.* **12** 3936
- [10] LeBeau J M and Stemmer S 2008 *Ultramicroscopy* **108** 1653
- [11] Findlay S D and LeBeau J M 2013 *Ultramicroscopy* **124** 52
- [12] Katz-Boon H, Rossouw C J, Dwyer C and Etheridge J 2013 *Ultramicroscopy* **124** 61